

EEG low-resolution brain electromagnetic tomography (LORETA) in Huntington's disease

Annamaria Painold · Peter Anderer · Anna K. Holl ·
Martin Letmaier · Gerda M. Saletu-Zyhlarz ·
Bernd Saletu · Raphael M. Bonelli

Received: 13 May 2010/Revised: 21 November 2010/Accepted: 25 November 2010
© Springer-Verlag 2010

Abstract Previous studies have shown abnormal electroencephalography (EEG) in Huntington's disease (HD). The aim of the present investigation was to compare quantitatively analyzed EEGs of HD patients and controls by means of low-resolution brain electromagnetic tomography (LORETA). Further aims were to delineate the sensitivity and utility of EEG LORETA in the progression of HD, and to correlate parameters of cognitive and motor impairment with neurophysiological variables. In 55 HD patients and 55 controls a 3-min vigilance-controlled EEG (V-EEG) was recorded during midmorning hours. Power spectra and intracortical tomography were computed by LORETA in seven frequency bands and compared between groups. Spearman rank correlations were based on V-EEG and psychometric data. Statistical overall analysis by means of the omnibus significance test demonstrated significant ($p < 0.01$) differences between HD patients and controls. LORETA theta, alpha and beta power were decreased from early to late stages of the disease. Only advanced disease stages showed a significant increase in delta power, mainly in the right orbitofrontal cortex. Correlation analyses revealed that a decrease of alpha and theta power correlated significantly with increasing cognitive and motor decline. LORETA proved to be a sensitive

instrument for detecting progressive electrophysiological changes in HD. Reduced alpha power seems to be a trait marker of HD, whereas increased prefrontal delta power seems to reflect worsening of the disease. Motor function and cognitive function deteriorate together with a decrease in alpha and theta power. This data set, so far the largest in HD research, helps to elucidate remaining uncertainties about electrophysiological abnormalities in HD.

Keywords Huntington's disease (HD) · Electroencephalography (EEG) · Low-resolution brain electromagnetic tomography (LORETA) · Power spectral analysis · Correlation analysis · Stages of the disease

Introduction

Huntington's disease (HD), a relentlessly progressive neurodegenerative disorder, is characterized by a clinical triad of psychiatric, cognitive, and motor disturbances. The underlying defect of HD is a pathologically elongated gene resulting from a base triplet elongation (CAG) on chromosome 4. This gene produces a protein called huntingtin which leads to neural apoptosis, especially in the striatum of the basal ganglia.

Recent evidence from neuroimaging studies suggests that neurodegenerative changes in HD extend to cortical gray-matter and cerebral white-matter regions. This is seen mainly in later stages of the disease, but findings are equivocal [1–6]. Furthermore, there is a high variability of cortical neuronal loss and volume changes in HD [1, 2, 5–11]. Several studies have shown a relation between measures of structural neuroimaging and disease duration, severity of dementia, severity of movement disorder, cognitive performance and/or functional capacity [5, 7, 8, 12–14].

A. Painold (✉) · A. K. Holl · M. Letmaier
Department of Psychiatry, Medical University of Graz,
Auenbruggerplatz 31, 8036 Graz, Austria
e-mail: annamaria.painold@medunigraz.at

P. Anderer · G. M. Saletu-Zyhlarz · B. Saletu
Department of Psychiatry and Psychotherapy, Medical
University of Vienna, Vienna, Austria

R. M. Bonelli
Sigmund Freud University Vienna, Vienna, Austria

The clinical relevance of electrophysiological tests in patients with HD has already been discussed by previous authors [15]. In their study, increasing alterations of somatosensory evoked potentials and blink reflexes were found in the follow-up of HD patients. But routine EEGs have also been reported as abnormal [16–25]. EEG patterns differ extensively among HD patients, but the most frequent electroencephalographic abnormality described in HD is an amplitude reduction or suppression of alpha activity [16–19]. Even in the EEG of preclinical mutation carriers for HD, reduced alpha activity was found [19].

In recent years only four quantitative EEG studies focused on routine EEG alterations in the course of HD. Shista et al. [20] reported a reduction of the EEG amplitude, which did not correlate with psychometric findings. However, other authors found significant correlations between increased theta and reduced alpha power and the clinical stage of dementia [16]. In another study disease duration was not correlated with any quantified EEG power measures, but the EEG of HD patients was generally characterized by a reduction in alpha and theta power and by an increase in delta and beta power [17]. The severity of neurological impairment was correlated with increased beta power and faster delta frequency, and poor cognitive performance was correlated with reductions in delta power, less theta power, reduced alpha power and increased beta power over frontal and temporal regions [17]. On the other hand, using artificial neural networks Tommaso et al. [19] reported that absolute alpha power was not correlated with cognitive decline.

In earlier studies, sample size was limited to a maximum of 16 HD patients. Moreover, the number of HD patients used to outnumber that of age-matched controls. Due to the alterations observed in the EEG of aged people [26–28], EEG evaluations should be conducted with an adequate number of age- and sex-matched controls.

Previous investigations of EEG in other neurodegenerative disorders has also revealed a disturbed functional brain state. EEG represents a brain imaging tool capable of identifying the earliest signs of brain dysfunction in subjects who go on to decline to mild cognitive impairment or convert to dementia, characterized by increased theta power [29]. Furthermore, previous studies have consistently demonstrated the relationship of increased delta and/or theta power to the severity and progression of dementia [e.g., 30–38]. A prominent decrease in alpha and/or beta power in cognitive decline has also been reported [e.g., 37–41]. Saletu et al. interpreted their neurophysiological findings of increased delta/theta power and additional decreased alpha and beta power as a deterioration of vigilance in dementia [39, 40].

EEG tomography techniques such as LORETA have been developed in order to identify brain regions involved

in neuro-psychiatric disorders. Since the progression of both neurological and cognitive impairment is slow in HD, general categorization of EEG aberrations may not reach sufficient sensitivity for the detection and localization of abnormalities. EEG tomography allows a detection of dysfunction that is more sensitive than that provided by the common EEG. LORETA computes a unique three-dimensional electrical source distribution by assuming that the smoothest of all possible inverse solutions is the most plausible, which is consistent with the assumption that neighbouring neurons are simultaneously and synchronously active [42, 43]. In LORETA the solution space is restricted to cortical gray matter and the hippocampus—as determined in the digitized Probability Atlas (Brain Imaging Center, Montreal Neurological Institute) based on the Talairach human brain atlas. The localization property of LORETA and the electrophysiological and neuroanatomical constraints used by LORETA have been criticized by some authors [44–46]. However, numerous studies provide validation for LORETA [e.g., 47–50]. Thus, LORETA, a now widely accepted, low-cost and non-invasive diagnostic tool, combines the high time resolution of the EEG with a source localization method that permits three-dimensional tomography of brain electrical activity. So far, LORETA has been used only twice in HD. Tommaso et al. [51] examined the contingent negative variation in 14 mildly demented HD patients, and Beste et al. [52] investigated executive functions related to response inhibition in 13 HD patients by using event-related potentials and LORETA.

The aim of the present study was (1) to detect abnormalities in spontaneous vigilance-controlled cortical activity in HD patients as compared with controls using LORETA, (2) to delineate the sensitivity and utility of LORETA in the progression of HD, hypothesizing that LORETA is able to distinguish early from late stages of HD by identifying and localizing different brain regions predominantly involved in the progression of the disease, and (3) to correlate parameters of cognitive and motor impairment with neurophysiological alterations measured by LORETA.

Methods

Subjects

Fifty-five patients (33 males, 22 females), aged between 20 and 69 years ($M = 45.44$, $SD = 12.33$) with the genetic diagnosis of HD were included in the study. EEG data on 16 additional patients had been acquired but were not included in the statistical analysis due to incorrigible movement artefacts. All patients were inpatients,

symptomatic, and suffered from mild to severe motor and cognitive symptoms (Unified Huntington's Disease Rating Scale (UHDRS) [53] motor section: $M = 36.60$, $SD = 17.76$; Mini-Mental State Examination (MMSE) [54]: $M = 19.95$, $SD = 4.69$). The mean duration of the disease was 4.07 years ($SD = 3.46$). HD stages were graded according to Shoulson's clinical stages [55]. At stage 1, patients clinically show minimal impairment and function at their usual level; at stage 5 patients are severely affected, suffer from pronounced motor and cognitive impairment and require institutional care. Twenty-one of our patients were in stage 1, 13 patients in stage 2, 17 patients in stage 3 and 4 patients were in stage 4. Patients in stages 3 and 4 were combined for statistical analyses. Due to severe movement artefacts no EEGs of stage 5-patients could be included in the study.

Twenty HD patients were drug-free (11 males, 9 females; mean age: 41.37 ± 9.15 years), 35 took medication (22 males, 13 females; mean age: 49.64 ± 13.23 years). Any medication taken by the patients over the previous months was noted and patients with benzodiazepines were not included in the study. To treat severe choreatic movements, eight patients received antipsychotics (tiapride, risperidone, olanzapine or amisulpride). For the treatment of symptoms of depression citalopram, sertraline, venlafaxine, mirtazapine or trazodone were used in 12 HD patients. Fifteen patients received a combination of these antidepressants and antipsychotics. The 20 drug-free patients either suffered only from mild symptoms or refused medication.

Sample characteristics of the HD patients are summarized in Table 1.

Patients were age- and sex-matched with 55 drug-free healthy controls (33 males, 22 females), aged between 20 and 69 years ($M = 45.51$, $SD = 12.63$), that had been recruited by advertisements. Controls displayed no physical, neurological or mental illness.

The study was approved by the local ethics committee. Informed consent was obtained.

Recording and analysis of the EEG

During the EEG recordings, subjects were instructed to sit comfortably and close their eyes. A 3-min vigilance-controlled EEG (V-EEG) was obtained at 11 a.m. with a 21-channel Nihon Kohden 4421 G polygraph (time constant: 0.3 s, high frequency response: 35 Hertz (Hz); amplification: approximately 20,000 times; maximal noise level: 2 μ V peak to peak). During the V-EEG recording the technician kept the patients alert. Gold electrodes were attached to the scalp according to the international 10/20 system. Nineteen EEG channels (Fp1, Fp2, F7, F3, Fz, F4, F8, T3, C3, Cz, C4, T4, T5, P3, Pz, P4, T6, O1 and O2 to averaged mastoids, monopolar montage) as well as the vertical and horizontal electro-oculographic recordings were digitized on-line with a sampling frequency of 102.4 Hz. Artefact-free 5 s epochs were selected after minimizing ocular artefacts by regression analysis in the time domain by an automatic artefact identification method with subsequent visual control [56]. Spectral analyses were performed for 5 s epochs (512 sample points), resulting in a frequency resolution of 0.2 Hz [57]. Since different EEG frequencies reflect different functions, data were digitally filtered into seven frequency bands according to Kubicki [58]: delta (1.5–6 Hz), theta (6–8 Hz), alpha-1 (8–10 Hz), alpha-2 (10–12 Hz), beta-1 (12–18 Hz), beta-2 (18–21 Hz), beta-3 (21–30 Hz).

The first published version of LORETA was used to estimate the three-dimensional intracerebral current density distribution [42]. The three-shell spherical head model [59] was registered to the human brain Talairach atlas [60] available as a digitized MRI from the McConnell Brain Imaging Centre, Montréal Neurological Institute, McGill University. The EEG electrode coordinates were used for

Table 1 Sample characteristics of the Huntington's disease patients

	Stage 1	Stage 2	Stage 3 and 4	All patients
Patients (<i>n</i>)	21	13	21	55
Sex (male/female)	11/10	8/5	14/7	33/22
Age in years, mean (SD)	39.62 (10.10)	49.28 (12.82)	48.89 (12.34)	45.44 (12.33)
Duration of disease in years, mean (SD)	1.42 (1.62)	3.32 (1.60)	7.14 (3.18)	4.07 (3.46)
UHDRS (0–124), mean (SD)	19.61 (7.44)	36.73 (7.12)	53.46 (9.77)	36.60 (17.76)
MMSE (30–0), mean (SD)	23.18 (3.81)	20.12 (3.60)	16.55 (3.76)	19.95 (4.69)
AD (<i>n</i>)	5	5	2	12
AP (<i>n</i>)	3	2	3	8
AD and AP (<i>n</i>)	1	3	11	15

AD antidepressants, AP antipsychotics

registration between spherical and realistic head geometry [61]. Based on the digitized Probability Atlas corresponding to the digitized MRI and also available from the McConnell Brain Imaging Centre (Montréal Neurological Institute, McGill University), a voxel was included in the solution space if its probability of being gray matter was higher than 33%, and higher than its probability of being either white matter or cerebrospinal fluid. Finally, the solution space was restricted to cortical and hippocampal gray matter. The EEG lead field was computed numerically with the boundary element method [43]. For each recording, LORETA spectral powers of six 5 s epochs of artefact-free, vigilance-controlled EEG were averaged. Thus, the presented LORETA images represent 2,394 voxels with a spatial resolution of 7 mm [43].

Statistical analysis

To display the differences between HD patients and controls, independent sample t tests were performed for log-transformed LORETA power. These voxel-by-voxel t values were displayed as statistical parametric maps (SPMs). To correct for multiple comparisons, a non-parametric single-threshold test was applied on the basis of the theory for randomization and permutation tests developed by Holmes et al. [62] for functional mapping experiments. Thus, the omnibus null hypothesis of no activation anywhere in the brain was rejected if at least one t value (i.e. t_{\max}) was above the critical threshold t_{crit} for $p = 0.01$ determined by 5,000 randomizations. Voxels in Talairach space with t values above this critical 0.01 threshold were considered as the region of activation [63]. In order to constitute a significant suprathreshold region, the number of voxels had to be ≥ 138 out of 2,394 (binomial test) [64]. On the basis of the Structure-Probability Maps Atlas, the number of significant voxels in each lobe (frontal, parietal, occipital, temporal, limbic and sub-lobar), gyrus, and Brodmann area (BA) of the left and the right hemisphere was computed.

The UHDRS motor score and the MMSE score were selected for correlation analysis between motor impairment as well as cognitive impairment and neurophysiological variables. Spearman rank correlations determined by means of the SPSS 17.0 software package were based on V-EEG and psychometric data obtained in HD patients on the day of the EEG examination. The resulting voxel-by-voxel correlation coefficients were displayed as SPMs. To correct for the α -inflation due to multiple tests, an omnibus significance test based on the binomial theorem was performed ($\alpha = 0.05$) [64]. Thus, to reject the global null hypothesis, more than 33 out of the total of 2,394 test results had to be significant at $p < 0.01$. Again, on the basis of the Structure-Probability Maps Atlas, the number

of significant voxels in each lobe (frontal, parietal, occipital, temporal, limbic and sub-lobar), gyrus, and Brodmann area (BA) of the left and the right hemisphere was computed.

Results

LORETA differences between 55 HD patients and controls

Statistical overall analysis by means of the omnibus significance test demonstrated significant differences ($p < 0.01$) in the V-EEG between patients and controls. In the delta band 433 out of 2,394 voxels showed significant current source density differences. In the theta band the number of voxels showing significant differences was 1,811, in the alpha-1 band 2,394, in the alpha-2 band 2,304, in the beta-1 band 2,048, in the beta-2 band 2,199 and in the beta-3 band 2,184 (Table 2, Fig. 1).

In detail, in the V-EEG of HD patients, an increase in delta LORETA power was observed which affected the right hemisphere more than the left (346 vs. 87 voxels). The highest number of significant voxels was found in right frontal cortical areas, involving more than half of the right frontal lobe with emphasis on the orbitofrontal area (BA 10, 11, 47). The maximum difference ($t_{\max} = 4.8$) was seen in the right BA 11 of the inferior frontal gyrus (Table 2).

Analysis of the other six frequency bands (theta, alpha-1, alpha-2, beta-1, beta-1 and beta-3 power) showed significant ($p < 0.01$) decreases in LORETA power. The alpha attenuation was significant all over the cortex and involved all possible voxels. The decrease in LORETA theta and beta power was also significant all over the cortex; however, in frontal, temporal, parietal, limbic and sub-lobar areas, nearly all possible voxels were involved (>80%), whereas in occipital cortical areas, only 30% or fewer of all possible voxels were involved (Fig. 1).

LORETA differences between 20 drug-free HD patients and controls

To investigate whether medication had a significant effect on the V-EEG the above analysis was computed again, including only the 20 drug-free patients and 20 age- and sex-matched controls. Similar to the results of the comparison of all 55 HD patients and controls, a significant increase in LORETA delta power and a significant decrease in LORETA theta, alpha and beta power was found ($p < 0.01$). Topographic distribution was also similar to that seen in the comparison between all patients and controls (Table 2).

Table 2 Differences between all HD patients and controls ($n = 2 \times 55$) and between drug-free patients and controls ($n = 2 \times 20$) as well as patients with medication and controls ($n = 2 \times 35$)

	Differences between all HD patients and controls ($n = 2 \times 55$)			Differences between drug-free patients and controls ($n = 2 \times 20$)			Differences between patients with medication and controls ($n = 2 \times 35$)		
	t_{max}	N _{sig} LH/RH	Brain region	t_{max}	N _{sig} LH/RH	Brain region	t_{max}	N _{sig} LH/RH	Brain region
Delta 1.5–6 Hz	4.8	87/346	F _{R>L}	3.2	101/446	F _{R>L}	3.6	79/238	F _{R>L}
Theta 6–8 Hz	-7.4	1,044/767	F, T, P, L, SI, O*	-5.9	877/501	F, T, P, L, SI	-5.1	786/591	F, T, P, L, SI
Alpha-1 8–10 Hz	-9.0	1,205/1,189	Total cortex	-6.0	1,157/1,165	Total cortex	-6.8	1,205/1,184	Total cortex
Alpha-2 10–12 Hz	-8.6	1,175/1,129	Total cortex	-5.5	674/315	F, T, P, L, SI	-6.6	1,115/993	Total cortex
Beta-1 12–18 Hz	-8.1	1,057/991	F, T, P, L, SI, O*	-5.8	802/608	F, T, P, L, SI	-6.0	917/781	F, T, P, L, SI, O*
Beta-2 18–21 Hz	-8.1	1,087/1,112	F, T, P, L, SI, O*	-5.5	897/869	F, T, P, L, SI	-7.0	1,031/805	F, T, P, L, SI, O*
Beta-3 21–30 Hz	-10.0	1,091/1,093	F, T, P, L, SI, O*	-6.6	1,017/963	F, T, P, L, SI	-9.1	1,096/1,095	F, T, P, L, SI, O*

The omnibus significance is based on binomial tests for each frequency band. Maximal t values (t_{max}) and the number of significant voxels (N_{sig} out of 2,394 voxels) are given for LH (left hemisphere)/RH (right hemisphere). Predominantly brain regions (F frontal lobe, T temporal lobe, P parietal lobe, O occipital lobe, L limbic lobe, SI sub-lobar; index_L indicates left lateral, index_R right lateral) are given. Positive t values indicate increases of a particular frequency band in HD patients as compared to normal controls, negative t values indicate decreases

* Brain region with less than 30% significant voxels

LORETA differences between 35 HD patients with medication and controls

The above analysis was performed once again, including the 35 HD patients with medication and 35 age- and sex-matched controls. Statistical overall analysis by means of the omnibus significance test again demonstrated significant differences ($p < 0.01$) in the V-EEG between patients with medication and controls. An increase in LORETA delta power and a decrease in LORETA theta, alpha and beta power was found. Changes in LORETA power and their topographic distribution were again similar to the results observed in the comparison between all patients and controls (Table 2).

LORETA differences between 21 HD patients in stage 1 and controls

Statistical overall analysis by means of the omnibus significance test demonstrated significant differences ($p < 0.01$) in the V-EEG between patients in stage 1 and controls in the theta, alpha and beta band. In the V-EEG there was a widespread decrease in LORETA theta, alpha and beta power in frontal, temporal, parietal, limbic and sub-lobar areas. Only the decrease in alpha-1 power also affected the occipital lobe (Fig. 2). The maximal differences for LORETA theta, alpha and beta power were seen in frontal and temporal areas. The decrease in LORETA power was more prominent over the left hemisphere (Table 3).

LORETA differences between 13 HD patients in stage 2 and controls

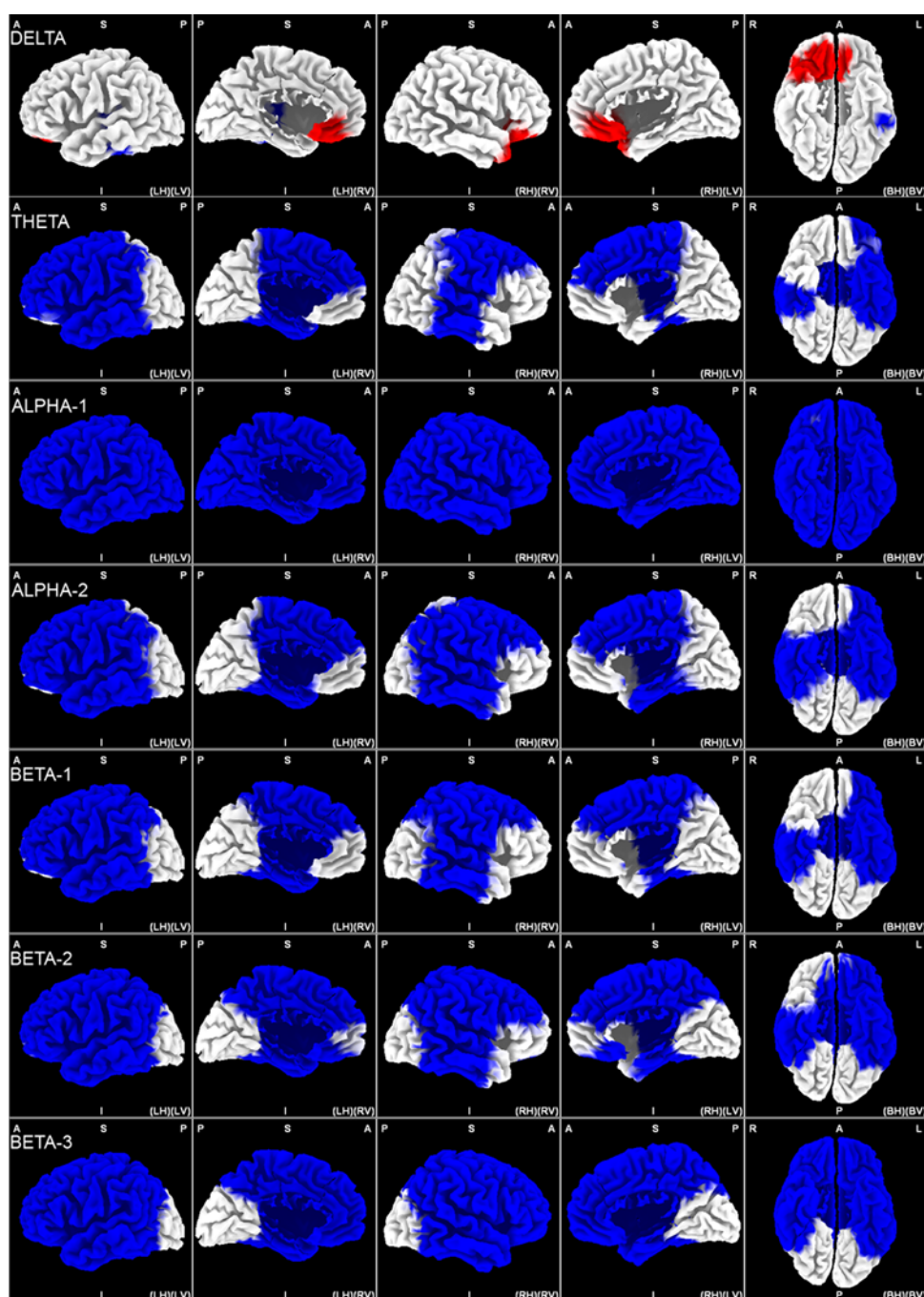
Similar to the results of the comparison between HD patients in stage 1 and normal controls, in stage-2 patients there was also a significant ($p < 0.01$) decrease in LORETA theta, alpha and beta power, which affected frontal, temporal, parietal, limbic and sub-lobar areas. Only LORETA alpha-2 power was also decreased in occipital cortices. The maximal differences for LORETA theta, alpha and beta power were seen in frontal and temporal areas. If not almost all voxels were affected, the decrease in LORETA power was again more prominent in left hemispheric voxels (Table 3).

LORETA differences between 21 patients in stage 3 and 4 and controls

For statistical analysis, 17 stage-3 patients and 4 stage-4 patients were combined.

Statistical analysis demonstrated significant differences ($p < 0.01$) in the V-EEG between patients in stage 3 and 4 and controls in all frequency bands. In the delta band, 333

Fig. 1 LORETA differences in 7 frequency bands between all HD patients and controls during the vigilance-controlled recording ($n = 2 \times 55$). Images depicting statistical parametric maps seen from different perspectives are based on voxel-by-voxel t values ($p < 0.01$) of differences between the two groups for delta, theta, alpha-1 and alpha-2, beta-1, beta-2 and beta-3 bands. Structural anatomy is shown in gray scale (A anterior, P posterior, S superior, I inferior, LH left hemisphere, RH right hemisphere, BH both hemispheres, LV left view, RV right view, BV bottom view). Red colours indicate increases, blue colours decreases, as compared with controls (t_{crit} for delta: 3.42; theta: 3.23; alpha-1: 3.06; alpha-2: 3.15; beta-1: 3.17; beta-2: 3.16 and beta-3: 3.21). Delta power increases in frontal regions of the right hemisphere. Alpha power is reduced all over the cortex. The decrease in theta and beta power is widespread in every lobe, only occipital areas are less than 30% affected



out of 2,394 voxels showed significant current source density differences. In the theta band, the number of voxels showing significant differences was 985, in the alpha-1 band 2,287, in the alpha-2 band 771, in the beta-1 band 163, in the beta-2 band 553 and in the beta-3 band 1,176 (Table 3 and Fig. 2).

In detail, there was an increase in LORETA delta power in the frontal lobe, involving more right than left hemispheric voxels. In more than half of the right frontal lobe the increase in LORETA delta power was significant, whereas the highest number of significant voxels were

found in the right orbitofrontal cortex (OFC) and anterior cingulate cortex (ACC) (BA 10, 11, 47 and 25). Fewer significant voxels were found in the right BA 9 and 46 of the dorsolateral prefrontal cortex (DLPFC). The maximal difference ($t_{max} = 3.6$) was seen in the right BA 11 of the inferior frontal gyrus.

Analysis of the other six frequency bands (theta, alpha-1, alpha-2, beta-1, beta-2 and beta-3 power) showed significant ($p < 0.01$) decreases in LORETA power. The decrease in alpha-1 power affected the whole cortex; the same was true for the decrease in theta and alpha-2 power,

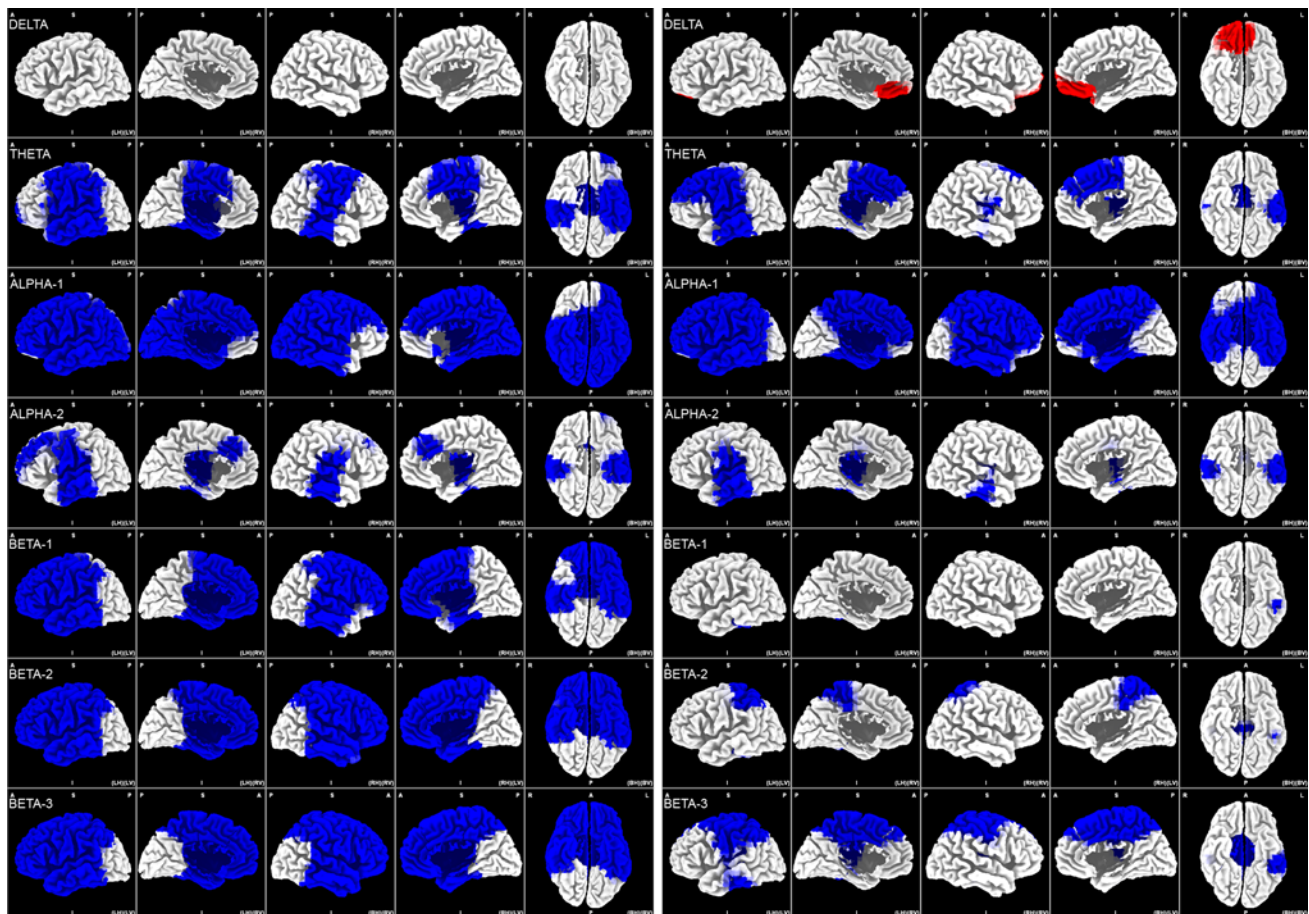


Fig. 2 LORETA differences in seven frequency bands between HD patients in stage 1 and normal controls ($n = 2 \times 21$) on the left side and between HD patients in stage 3 and 4 and normal controls ($n = 2 \times 21$) on the right side during the vigilance-controlled recording. For a technical description of the statistical parametric maps see Fig. 1. t_{crit} for patients in stage 1 for delta: 3.57; theta: 3.42; alpha-1: 3.27; alpha-2: 3.00; beta-1: 3.39; beta-2: 3.40 and beta-3: 3.50 and t_{crit} for patients in stage 3 and 4 for delta: 3.41; theta: 3.40; alpha-1: 3.23; alpha-2: 3.41; beta-1: 3.51; beta-2: 3.43 and beta-3: 3.55. Delta power is significantly increased in prefrontal regions of

with the exception of occipital areas. LORETA beta-1 power was significantly attenuated over temporo-parietal cortices, beta-2 power over high-frontal, limbic and temporo-parietal regions and beta-3 power was decreased over frontal, temporal, parietal and limbic cortices. The maximal differences for LORETA theta, alpha and beta power were seen in temporal and parietal areas. The decrease in LORETA power was again more pronounced in left hemispheric voxels (Table 3, Fig. 2).

Correlations between the UHDRS motor score and LORETA power in 20 drug-free patients

Due to the higher sensitivity of correlation analyses to the influences of medication, these calculations were computed

the right hemisphere in stage 3 and 4. Theta, alpha and beta power are significantly decreased in stage 1 and in stage 3 and 4. In both early and advanced stages, alpha-1 power is reduced over the whole cortex, while the decrease in theta and alpha-2 power is not seen over the occipital cortex. In stage-1 patients the decrease in all beta bands is found in frontal, temporal, parietal and limbic regions. In stage 3 and 4 the decrease in beta power is more localized, with beta-1 power being decreased only in temporal and parietal regions and beta-2 power in temporal, parietal, limbic and high-frontal regions. Beta-3 power is reduced in all regions except the occipital regions

for the 20 drug-free patients only. Spearman rank correlations between the UHDRS motor score and LORETA power measured in seven frequency bands demonstrated significant negative correlation in the theta and alpha-2 frequency bands: the lower the power in these frequency bands, the higher the UHDRS score. The omnibus significance test showed that the number of significant voxels out of 2,394 possible voxels was 170 for theta and 537 for alpha-2 ($p < 0.01$, binomial test). Regarding theta power, the highest negative correlation coefficient ($r = -0.54$) was observed in the medial frontal gyrus in BA 9 ($X = -10$, $Y = 38$, $Z = 29$). Concerning alpha-2 power, the highest negative correlation coefficient ($r = -0.52$) was observed in the ACC in BA 25 ($X = -3$, $Y = -11$, $Z = -6$). Significant correlations were found mainly in the

Table 3 Differences between HD patients in stage 1 and normal controls ($n = 2 \times 21$) and between patients in stage 2 and normal controls ($n = 2 \times 13$) as well as patients in stage 3 and 4 and normal controls ($n = 2 \times 21$)

	Differences between patients in stage 1 and normal controls ($n = 2 \times 21$)			Differences between patients in stage 2 and normal controls ($n = 2 \times 13$)			Differences between patients in stage 3 and 4 and normal controls ($n = 2 \times 21$)					
	t_{max}	N_{SIG}	LH/RH	Brain region	t_{max}	N_{SIG}	LH/RH	Brain region	t_{max}	N_{SIG}	LH/RH	Brain region
Delta 1.5–6 Hz												
Theta 6–8 Hz	-5.9	951/631		F _{L>R} , T _{L>R} , P, L, SI	-3.1	243/130		F _{L>R} , T _{L>R} , P, L, SI	3.6	74/259		F _{R>L}
Alpha-1 8–10 Hz	-5.9	1,205/1,062		Total cortex	-4.3	1,002/885		F _{L>R} , T, P, L, SI _{L>R}	-4.5	680/305		F _{L>R} , T _{L>R} , P, L, SI _{L>R}
Alpha-2 10–12 Hz	-5.6	678/412		F _{L>R} , T _{L>R} , P, L, SI _{L>R}	-6.3	1,201/1,189		Total cortex	-5.3	1,158/1,129		Total cortex
Beta-1 12–18 Hz	-7.1	928/896		F, T, P, L, SI	-7.1	1,017/933		F _{L>R} , T, P, L, SI	-3.9	510/261		F _{L>R} , T _{L>R} , P, L _{L>R} , SI
Beta-2 18–21 Hz	-7.7	1,009/986		F, T, P, L, SI	-9.4	1,066/1,044		F, T, P, L, SI	-2.9	126/37		T _{L>R} , P _L
Beta-3 21–30 Hz	-9.3	1,062/1,017		F, T, P, L, SI	-8.6	1,073/1,079		F, T, P, L, SI	-3.3	324/229		T, P _{L>R} , F _{L>R} , L, SI

The omnibus significance is based on binomial tests for each frequency band. Maximal t values (t_{max}) and the number of significant voxels (N_{SIG} out of 2,394 voxels) are given for LH (left hemisphere)/RH (right hemisphere). Predominant brain regions (F frontal lobe, T temporal lobe, P parietal lobe, O occipital lobe, L limbic lobe, SI sub-lobar; index_L indicates left lateral, index_R right lateral) are given. Positive t values indicate increases of a particular frequency band in HD patients as compared to normal controls, negative t values indicate decreases

frontal and limbic lobes of both hemispheres, and for alpha-2 power also in the occipital lobes (Fig. 3).

Correlations between the MMSE score and LORETA power in 20 drug-free patients

Spearman rank correlations between the MMSE score and LORETA power measured in seven frequency bands demonstrated a significant positive correlation in the alpha-1 frequency range: the lower the power in this frequency band, the lower the MMSE score. The omnibus significance test demonstrated that out of a total of 2,394 voxels, 232 voxels showed significant correlations in the alpha-1 band ($p < 0.01$, binomial test). The highest positive correlation coefficient ($r = 0.55$) was observed in the superior frontal gyrus in BA 9 ($X = 11, Y = 59, Z = 29$). Correlations were found mainly in the frontal lobe of the right hemisphere and the limbic lobes of both hemispheres (Fig. 4).

Discussion

To our knowledge, this is the first application of LORETA to artefact-free EEG recordings obtained in HD patients and controls in a vigilance-controlled state with eyes closed. The present EEG data were analysed by means of EEG LORETA following three approaches: (1) detection and computation of spatial distribution of abnormalities in vigilance-controlled cortical activity in HD, (2) differentiation between patients in early and late stages of the disease to delineate the sensitivity and utility of LORETA in the progression of HD, and (3) correlation analysis between neurophysiological alterations measured by LORETA and cognitive and motor impairment in HD.

As we are aware of the fact that the solution space of LORETA is restricted to cortical gray matter and the hippocampus, we were primarily interested in the utility and results of LORETA in a subcortical disease such as HD. HD is characterized by an accumulation of subcortical and cortical dysfunctions and a disruption of cortico-subcortical circuits. Current neuroimaging findings are not able to answer the questions as to when and in which exact area of the cerebral cortex meaningful neuronal loss is first observed. However, due to the extensive connections between the frontal lobes and subcortical structures, the frontal cortex and the basal ganglia are mainly seen as a functional unit in HD. For this reason it is of minor importance whether localized EEG power changes are caused by cortical or subcortical dysfunction. At present it is not possible to distinguish between an EEG pattern caused by a cortical lesion and an EEG pattern caused by a disruption of a cortico-subcortical circuit.

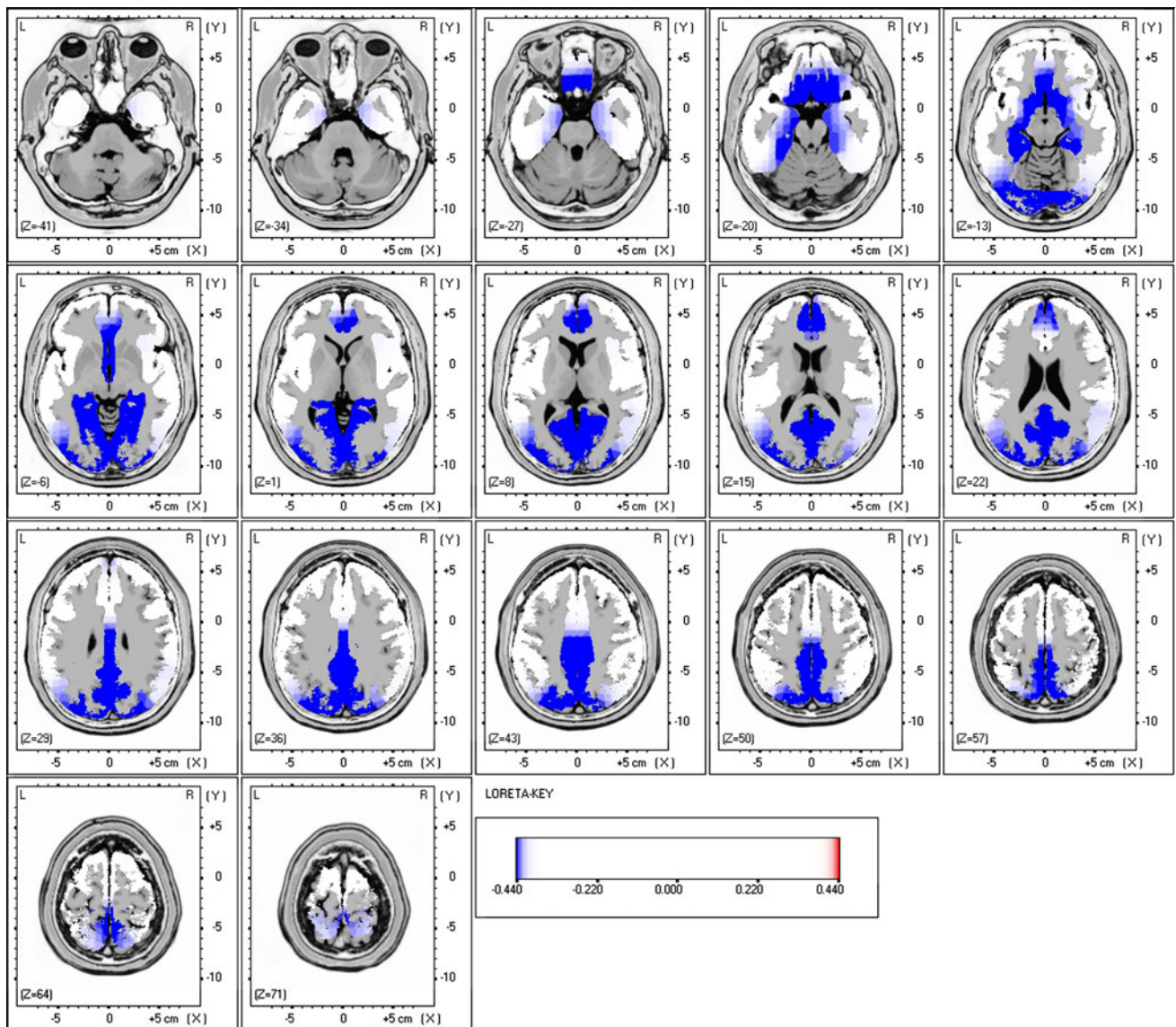


Fig. 3 LORETA slices on correlations between UHDRS motor score and alpha-2 power. *Horizontal* brain slices depicting statistical parametric maps are based on voxel-by-voxel Spearman rank correlation analysis between UHDRS motor score and alpha-2 power.

The colour key shows significant correlation coefficients (*blue* colours represent negative correlations at $p < 0.01$). The lower the alpha-2 power in the frontal, limbic and occipital lobes, the higher the UHDRS motor score

EEG power spectral values

In the whole group of 55 HD patients, a significant increase was found in LORETA delta power, mainly in the OFC of the right hemisphere, along with a global decrease in theta, alpha and beta power. HD patients showed a disturbed brain function characterized by inhibited frontal areas (increased delta power), while the whole cortex lacked normal routine and excitatory activity (decreased theta, alpha and beta power).

When the patients were separated according to different clinical stages of the disease, the significant increase in LORETA delta power in the right OFC was found only in

patients in stages 3 and 4. In addition to the lack of normal routine activity (decreased theta, alpha and beta power), which was also found in patients in earlier stages, these patients showed inhibited prefrontal areas.

Our findings of reduced alpha power confirm similar findings of previous EEG studies in HD [16–19] and in vascular (multi-infarct) dementia and Alzheimer's disease (AD) [37, 39, 40, 65]. The origin of the alpha rhythm is still unclear, but the abnormality may be associated with a dysfunction primarily affecting the cortex or a dysfunction of subcortical structures which modulate cortical activity, mainly the thalamus. The pathophysiological background in HD is the bilateral striatal atrophy, which leads to a

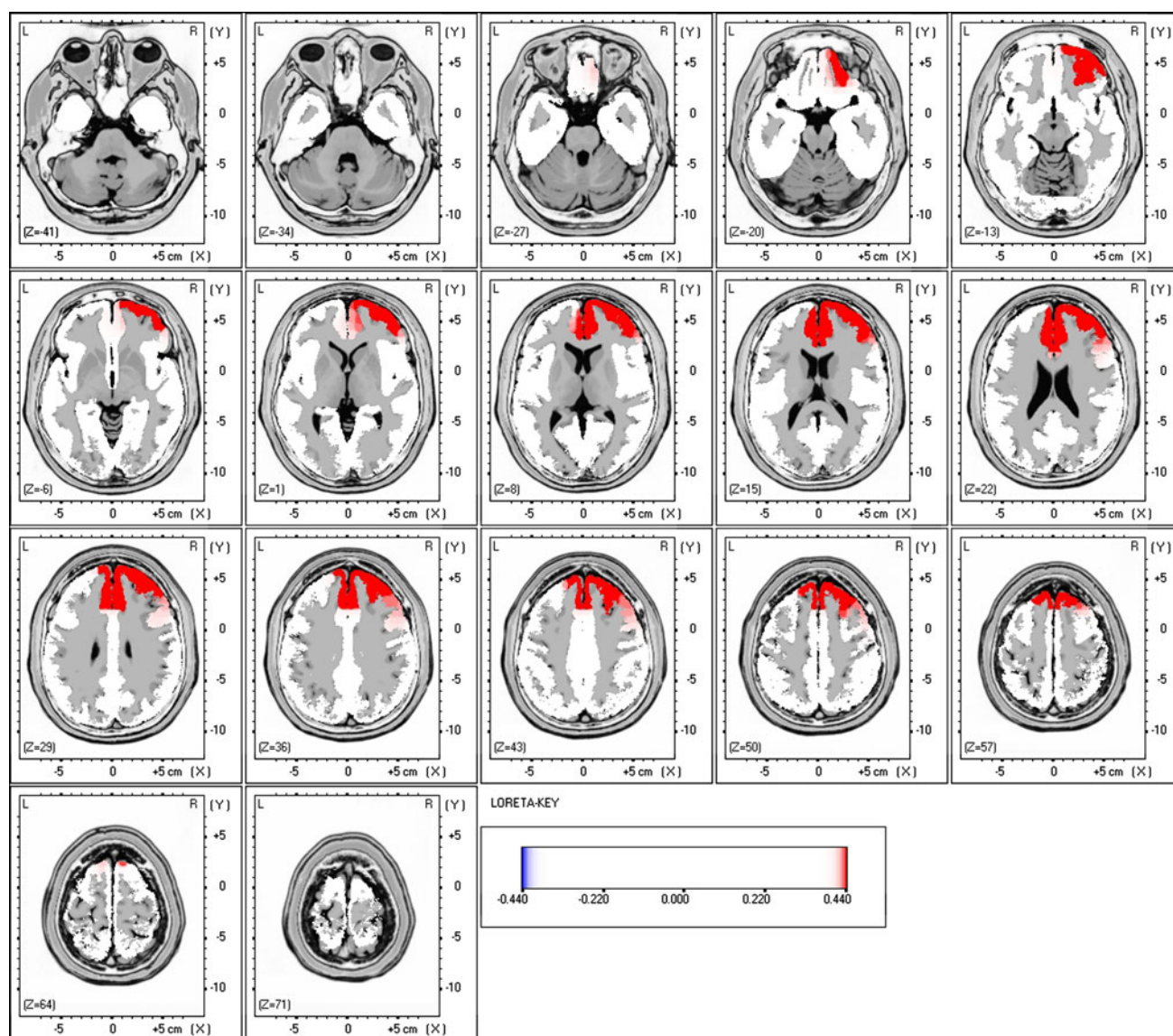


Fig. 4 LORETA slices on correlations between MMSE score and alpha-1 power. *Horizontal* brain slices depicting statistical parametric maps are based on voxel-by-voxel Spearman rank correlation analysis between MMSE score and alpha-1 power. The colour key shows

significant correlation coefficients (*red* colours represent positive correlations at $p < 0.01$). The lower the alpha-1 power in the right frontal lobe and both limbic lobes, the lower the MMSE score

disruption of the cortico-striato-thalamocortical circuits causing a decrease in thalamic alpha activity [66, 67]. Therefore, the results can be interpreted as an effect of an abnormal subcortical modulation of the alpha rhythm due to dysfunctional action of the thalamus on the cortical activities [18, 19, 67]. The decrease in alpha power in our patients was found all over the cortex, affecting nearly every voxel. Reduced alpha activity seems to be a typical and widespread trait marker of HD, from early to late stages of the disease.

The observed decrease in beta power has not yet been reported in HD, but adds to a possible understanding of our present findings, suggesting a deterioration of vigilance as a prominent neurophysiological finding in HD. Vigilance

was defined by Head [68] as the availability and grade of organization of man's adaptive behaviour, which in turn is dependent upon the dynamic state of the neuronal network. Indeed, the latter became measurable objectively and quantitatively by computerized analysing methods, initially by single-lead analysis [69, 70] and subsequently by EEG topography and tomography [39, 40, 42, 43]. Our results are in agreement with previous studies in patients with AD and vascular dementia [37, 39, 40], which also reported a decrease in alpha and beta power. In AD, the decrease in beta power was interpreted as a sign of compromised function of the affected brain areas [37]. Thus, it seems that dementing disorders generally lead to a decrease in beta

power, which is just opposite to normal aging where an increase in beta activity was found [27, 71–73]. The decrease in beta power in our study was prominent and—except in occipital cortical areas—highly significant all over the brain. The structural cause of this result might be a loss of cholinergic and glutamatergic neurons in the course of the disease [11].

Topographic distributions

The whole group of HD patients and patients in advanced stages (3 and 4) showed a localized increase in LORETA delta power in the right OFC as compared with healthy controls. An increase in delta power was already found by previous authors in HD [17] and other neurodegenerative disorders [29, 33, 37, 39, 74, 75]. The increase was most pronounced in the OFC (BA 10, 11 and 47), but the ACC (BA 25) and the DLPFC (BA 9, 46) were also affected. Several previous neuroimaging studies [7, 12, 76, 77], EEG studies [17] and necropsy investigations [9, 11] reported a dysfunction or deterioration of the frontal lobe in HD. Furthermore, frontal lobe atrophy seems to be characteristic for moderately affected, but not mildly affected, HD patients [7].

Neuroimaging studies on brain activation and functional connectivity suggest that interactions between prefrontal regions and between the prefrontal cortex and the basal ganglia are compromised in HD patients [77]. This is consistent with the existing knowledge on the neuropathology in HD and strongly supports the notion of deficits in prefrontal circuits [78–81]. Different parts of the frontal lobe are integrated in different circuits that link cortex, basal ganglia and thalamus [82, 83]. Main circuits are the motor circuit, which includes the primary and supplementary motor cortices that project to the putamen, the associative circuit between the DLPFC and the dorsolateral part of the caudate nucleus, the orbitofrontal circuit between the lateral OFC and the ventromedial caudate area and the limbic circuit between the anterior cingulate and the ventral striatum [80, 81].

Neuronal death in the caudate proceeds from dorsal to ventral and from medial to lateral areas, with the earliest alterations being seen in the medial paraventricular caudate, caudate tail, and dorsal putamen [84, 85]. Thus, in early HD, the associative loop should be dysfunctional, while the orbitofrontal loop and the limbic loop should remain intact. This is in line with our electrophysiological findings of an inhibited function of the OFC and ACC only in later stages of the disease. For the following reasons the previous interruption of the associative circuit may not become electrophysiologically significant over the DLPFC: According to Alper et al. [67, 86], the major site of delta generation is the OFC, which makes this region more

sensitive to changes in delta power. Furthermore, progressive deterioration and interruption of the reciprocal interconnections between the basal ganglia and the frontal cortex together with localized atrophic degenerations [7, 12], which are more prominent in later stages, may finally lead to the increase in delta power.

The ubiquitous decrease in theta, alpha and beta power reflects also very likely an accumulation of cortical structural impairment together with the alterations of the basal ganglia. Previous neuroimaging studies reported a widespread degeneration and heterogeneous regional thinning of the cortical ribbon [1, 2, 12] and global atrophy [6, 8] in the course of HD. To date it remains controversial whether cortical degeneration precedes or results from subtle striatal alterations in HD. Our results of early and stable electrophysiological dysfunctions support previous studies that reported early degeneration of the cerebral cortex [2, 5]. On the other hand, cortical areas of functional changes need not correspond to those of gray-matter atrophy and in this case, they are likely to reflect decreased output of the basal ganglia-thalamo-cortical circuits and compensatory recruitment of accessory pathways [87].

The occipital lobe seems to be an exception. From all power frequencies, only alpha power was found to be significantly reduced in these cortical areas. Alpha power is known to be the dominant frequency in occipital areas, which makes this frequency more sensitive to subtle alterations. The existing literature on the occipital lobe in HD is rare and equivocal, but our results support the assumption that occipital areas degenerate less or more slowly than other cortical areas [5, 11].

Huntington's disease is not thought to be a lateralized disease. Interestingly, differences in the results between the right and the left hemisphere were found. The increase in LORETA delta power was emphasized over right frontal regions, but the decreases in theta, alpha and beta power were more prominent over the left hemisphere. A few previous studies also reported about lateralized results, suggesting an earlier and more prominent affection of the left cortico-striatal system [2, 17, 88].

Correlation analyses

As EEG changes seem to be dynamic in progressive HD, correlation analyses between the MMSE score as well as the UHDRS motor score and LORETA power have been computed. In this study we found a significant negative correlation between the UHDRS motor score and LORETA power. The higher the UHDRS motor score, reflecting progressive motor impairment in HD patients, the less power in the theta and alpha-2 frequency band was found. Further analysis showed a significant positive correlation between the MMSE score and LORETA power. The lower

the power in the alpha-1 frequency band, the worse was the mental performance. Correlations were mainly found over the frontal and limbic lobes, and for alpha-2 power over the occipital lobes. Motor function and cognitive function deteriorate together with a decrease in alpha power, which seems to reflect the process of neurodegeneration. The correlation between decreased frontal and limbic theta power and higher motor impairment has not yet been reported, but the relationship of a decrease in alpha power to the progression of dementia confirms previous studies in HD [16, 17] and other neurodegenerative disorders [37–41].

Effect of medication

Twenty of the patients included in our study were drug-free, 35 patients were taking medication. The results of the whole group of patients are similar to those of the drug-free patients. The significant increase in LORETA delta power in the right OFC was found in 446 out of 2,394 voxels (drug-free patients) compared to 238 voxels (patients with medication) and 346 voxels (all patients). In each group the significant decrease in theta, alpha and beta power affected more than 1,000 out of 2,394 possible voxels. The topographic distribution of the significant results was similar in all groups. Putative effects of psychotropic drugs are dose-dependent, but sedative antidepressants and antipsychotics generally induce an increase of slow EEG activity and a decrease of alpha and beta power, while non-sedative antidepressants and antipsychotics increase alpha and alpha-adjacent beta-activity. In our patient sample medication did not affect the interpretation of the quantitative EEG differences between the group of HD patients and controls. EEG abnormalities in HD seem to be so strong that psychotropic drugs have no notable influences on them. Nevertheless, the more sensitive correlation analyses were computed for the drug-free patients only. These analyses are more susceptible to any faults or influences.

This study supplements previous EEG investigations in HD with a new method and new findings in a large cohort of patients. LORETA revealed a disturbed brain function in HD, characterized by inhibited frontal areas and a lack of normal routine and excitatory activity over the whole cortex. As hypothesized, LORETA is also a sensitive and useful measure for detecting progressive electrophysiological changes in the course of the disease. From early to late stages of the disease, patients showed a lack of theta, alpha and beta power. In later stages of the disease, patients demonstrated additional inhibited frontal areas (increased delta power). Reduced alpha power seems to be a stable trait marker of HD, whereas increased frontal delta power seems to reflect worsening of the disease. Correlation analyses revealed a decrease of theta and alpha power with

increasing cognitive decline and deterioration of motor function.

These data help to eliminate remaining uncertainties and ambiguities on electrophysiological abnormalities during HD manifestation and progression. We are aware of the fact that no preclinical mutation carriers are included in this study. Further LORETA investigations in gene mutation carriers for HD are of interest.

Acknowledgments The authors would like to express their thanks to Josef Diez, MD, and Franz Reisecker, MD, Department of Neurology, Barmherzige Brüder Hospital of Graz, for their cooperative assistance in this project. Furthermore, we thank Mag. Elisabeth Grätzhofer, Department of Psychiatry, Medical University of Vienna, for her valuable editorial assistance.

Conflict of interest The authors have no conflict of interest to declare.

References

1. Rosas HD, Koroshetz WJ, Chen YI, Skeuse C, Vangel M, Cudkovicz ME, Caplan K, Marek K, Seidman LJ, Makris N, Jenkins BG, Goldstein JM (2003) Evidence for more widespread cerebral pathology in early HD: an MRI-based morphometric analysis. *Neurology* 60:1615–1620
2. Rosas HD, Liu AK, Hersch S, Glessner M, Ferrante RJ, Salat DH, van der Kouwe A, Jenkins BG, Dale AM, Fischl B (2002) Regional and progressive thinning of the cortical ribbon in Huntington's disease. *Neurology* 58:695–701
3. Aylward EH, Li Q, Stine OC, Ranen N, Sherr M, Barta PE, Bylsma FW, Pearlson GD, Ross CA (1997) Longitudinal change in basal ganglia volume in patients with Huntington's disease. *Neurology* 48:394–399
4. Hasselbalch SG, Oberg G, Sorensen SA, Andersen AR, Waldeemar G, Schmidt JF, Fenger K, Paulson OB (1992) Reduced regional cerebral blood flow in Huntington's disease studied by SPECT. *J Neurol Neurosurg Psychiatry* 55:1018–1023
5. Kassubek J, Juengling FD, Kioschies T, Henkel K, Karitzky J, Kramer B, Ecker D, Andrich J, Saft C, Kraus P, Aschoff AJ, Ludolph AC, Landwehrmeyer GB (2004) Topography of cerebral atrophy in early Huntington's disease: a voxel based morphometric MRI study. *J Neurol Neurosurg Psychiatry* 75:213–220
6. Kassubek J, Bernhard Landwehrmeyer G, Ecker D, Juengling FD, Mueche R, Schuller S, Weindl A, Peinemann A (2004) Global cerebral atrophy in early stages of Huntington's disease: quantitative MRI study. *Neuroreport* 15:363–365
7. Aylward EH, Anderson NB, Bylsma FW, Wagster MV, Barta PE, Sherr M, Feeney J, Davis A, Rosenblatt A, Pearlson GD, Ross CA (1998) Frontal lobe volume in patients with Huntington's disease. *Neurology* 50:252–258
8. Halliday GM, McRitchie DA, Macdonald V, Double KL, Trent RJ, McCusker E (1998) Regional specificity of brain atrophy in Huntington's disease. *Exp Neurol* 154:663–672
9. Sotrel A, Paskevich PA, Kiely DK, Bird ED, Williams RS, Myers RH (1991) Morphometric analysis of the prefrontal cortex in Huntington's disease. *Neurology* 41:1117–1123
10. Hedreen JC, Peyser CE, Folstein SE, Ross CA (1991) Neuronal loss in layers V and VI of cerebral cortex in Huntington's disease. *Neurosci Lett* 133:257–261

11. Mann DM, Oliver R, Snowden JS (1993) The topographic distribution of brain atrophy in Huntington's disease and progressive supranuclear palsy. *Acta Neuropathol* 85:553–559
12. Rosas HD, Salat DH, Lee SY, Zaleta AK, Pappu V, Fischl B, Greve D, Hevelone N, Hersch SM (2008) Cerebral cortex and the clinical expression of Huntington's disease: complexity and heterogeneity. *Brain* 131:1057–1068
13. Starkstein SE, Brandt J, Bylsma F, Peyser C, Folstein M, Folstein SE (1992) Neuropsychological correlates of brain atrophy in Huntington's disease: a magnetic resonance imaging study. *Neuroradiology* 34:487–489
14. Starkstein SE, Brandt J, Folstein S, Strauss M, Berthier ML, Pearlson GD, Wong D, McDonnell A, Folstein M (1988) Neuropsychological and neuroradiological correlates in Huntington's disease. *J Neurol Neurosurg Psychiatry* 51:1259–1263
15. Lefaucheur JP, Bachoud-Levi AC, Bourdet C, Grandmougin T, Hantraye P, Cesaro P, Degos JD, Peschanski M, Lisovoski F (2002) Clinical relevance of electrophysiological tests in the assessment of patients with Huntington's disease. *Mov Disord* 17:1294–1301
16. Streletz LJ, Reyes PF, Zalewska M, Katz L, Fariello RG (1990) Computer analysis of EEG activity in dementia of the Alzheimer's type and Huntington's disease. *Neurobiol Aging* 11:15–20
17. Bylsma FW, Peyser CE, Folstein SE, Folstein MF, Ross C, Brandt J (1994) EEG power spectra in Huntington's disease: clinical and neuropsychological correlates. *Neuropsychologia* 32:137–150
18. Bellotti R, De Carlo F, Massafra R, de Tommaso M, Sciruicchio V (2004) Topographic classification of EEG patterns in Huntington's disease. *Neurol Clin Neurophysiol* 2004:37
19. de Tommaso M, De Carlo F, Difruscolo O, Massafra R, Sciruicchio V, Bellotti R (2003) Detection of subclinical brain electrical activity changes in Huntington's disease using artificial neural networks. *Clin Neurophysiol* 114:1237–1245
20. Sishta SK, Troupe A, Marszalek KS, Kremer LM (1974) Huntington's chorea: an electroencephalographic and psychometric study. *Electroencephalogr Clin Neurophysiol* 36:387–393
21. Scott DF, Heathfield KW, Toone B, Margerison JH (1972) The EEG in Huntington's chorea: a clinical and neuropathological study. *J Neurol Neurosurg Psychiatry* 35:97–102
22. Kassubek J, Juengling FD, Ecker D, Landwehrmeyer GB (2005) Thalamic atrophy in Huntington's disease co-varies with cognitive performance: a morphometric MRI analysis. *Cereb Cortex* 15:846–853
23. Margerison JH, Scott DF (1965) Huntington's chorea: clinical, EEG and neuropathological findings. *Electroencephalogr Clin Neurophysiol* 19:314–316
24. Foster DB, Bagchi BK (1949) Electroencephalographic observations in Huntington's chorea. *Electroencephalogr Clin Neurophysiol* 1:247–248
25. Painold A, Anderer P, Holl AK, Letmaier M, Saletu-Zyhlarz GM, Saletu B, Bonelli RM (2010) Comparative EEG mapping studies in Huntington's disease patients and controls. *J Neural Transm* 117:1307–1318
26. Babiloni C, Binetti G, Cassarino A, Dal Forno G, Del Percio C, Ferreri F, Ferri R, Frisoni G, Galderisi S, Hirata K, Lanuzza B, Miniussi C, Mucci A, Nobili F, Rodriguez G, Luca Romani G, Rossini PM (2006) Sources of cortical rhythms in adults during physiological aging: a multicentric EEG study. *Hum Brain Mapp* 27:162–172
27. Anderer P, Saletu B, Pascual-Marqui RD, Semlitsch HV (2000) EEG and ERP topography and tomography in normal aging. In: Saletu B, Krijzer F, Ferber G, Anderer P (eds) *Electrophysiological brain research in preclinical and clinical pharmacology and related fields—an update*. Facultas, Wien, pp 122–138
28. Van Sweden B, Wauquier A, Niedermeyer E (1999) Normal aging and transient cognitive disorders in the elderly. In: Niedermeyer E, Da Silva FL (eds) *Electroencephalography: basic principles, clinical applications and related fields*, 4th edn. Williams & Wilkins, Baltimore, pp 340–348
29. Prichep LS (2007) Quantitative EEG and electromagnetic brain imaging in aging and in the evolution of dementia. *Ann N Y Acad Sci* 1097:156–167
30. Prichep LS, John ER, Ferris SH, Reisberg B, Almas M, Alper K, Cancro R (1994) Quantitative EEG correlates of cognitive deterioration in the elderly. *Neurobiol Aging* 15:85–90
31. Brunovsky M, Matousek M, Edman A, Cervena K, Krajca V (2003) Objective assessment of the degree of dementia by means of EEG. *Neuropsychobiology* 48:19–26
32. Dierks T, Perisic I, Frolich I, Ihl R, Maurer K (1991) Topography of the quantitative electroencephalogram in dementia of the Alzheimer type: relation to severity of dementia. *Psychiatry Res* 40:181–194
33. Helkala EL, Laulumaa V, Soikkeli R, Partanen J, Soininen H, Riekkinen PJ (1991) Slow-wave activity in the spectral analysis of the electroencephalogram is associated with cortical dysfunctions in patients with Alzheimer's disease. *Behav Neurosci* 105:409–415
34. Rice DM, Buchsbaum MS, Starr A, Auslander L, Hagman J, Evans WJ (1990) Abnormal EEG slow activity in left temporal areas in senile dementia of the Alzheimer type. *J Gerontol* 45:M145–M151
35. John ER, Prichep LS, Fridman J, Easton P (1988) Neurometrics: computer-assisted differential diagnosis of brain dysfunctions. *Science* 239:162–169
36. Anderer P, Saletu B, Kloppe B, Semlitsch HV, Werner H (1994) Discrimination between demented patients and normals based on topographic EEG slow wave activity: comparison between z statistics, discriminant analysis and artificial neural network classifiers. *Electroencephalogr Clin Neurophysiol* 91:108–117
37. Gianotti LR, Kunig G, Lehmann D, Faber PL, Pascual-Marqui RD, Kochi K, Schreiter-Gasser U (2007) Correlation between disease severity and brain electric LORETA tomography in Alzheimer's disease. *Clin Neurophysiol* 118:186–196
38. Mattia D, Babiloni F, Romigi A, Cincotti F, Bianchi L, Sperli F, Placidi F, Bozzao A, Giacomini P, Floris R, Grazia Marciani M (2003) Quantitative EEG and dynamic susceptibility contrast MRI in Alzheimer's disease: a correlative study. *Clin Neurophysiol* 114:1210–1216
39. Saletu B, Anderer P, Saletu-Zyhlarz GM, Pascual-Marqui RD (2005) EEG mapping and low-resolution brain electromagnetic tomography (LORETA) in diagnosis and therapy of psychiatric disorders: evidence for a key-lock principle. *Clin EEG Neurosci* 36:108–115
40. Saletu B, Anderer P, Paulus E, Grunberger J, Wicke L, Neuhold A, Fischhof PK, Litschauer G (1991) EEG brain mapping in diagnostic and therapeutic assessment of dementia. *Alzheimer Dis Assoc Disord* 5(Suppl 1):S57–S75
41. Schreiter-Gasser U, Gasser T, Ziegler P (1994) Quantitative EEG analysis in early onset Alzheimer's disease: correlations with severity, clinical characteristics, visual EEG and CCT. *Electroencephalogr Clin Neurophysiol* 90:267–272
42. Pascual-Marqui RD, Michel CM, Lehmann D (1994) Low resolution electromagnetic tomography: a new method for localizing electrical activity in the brain. *Int J Psychophysiol* 18:49–65
43. Pascual-Marqui RD, Lehmann D, Koenig T, Kochi K, Merlo MC, Hell D, Koukkou M (1999) Low resolution brain electromagnetic tomography (LORETA) functional imaging in acute, neuroleptic-naive, first-episode, productive schizophrenia. *Psychiatry Res* 90:169–179

44. de Peralta Menendez RG, Andino SL (2000) Discussing the capabilities of Laplacian Minimization. *Brain Topogr* 13:97–104
45. Kincses WE, Braun C, Kaiser S, Elbert T (1999) Modeling extended sources of event-related potentials using anatomical and physiological constraints. *Hum Brain Mapp* 8:182–193
46. Michel CM, Grave de Peralta R, Lantz G, Gonzalez Andino S, Spinelli L, Blanke O, Landis T, Seeck M (1999) Spatiotemporal EEG analysis and distributed source estimation in presurgical epilepsy evaluation. *J Clin Neurophysiol* 16:239–266
47. Pascual-Marqui RD, Esslen M, Kochi K, Lehmann D (2002) Functional imaging with low-resolution brain electromagnetic tomography (LORETA): a review. *Methods Find Exp Clin Pharmacol* 24(Suppl C):91–95
48. Phillips C, Rugg MD, Friston KJ (2002) Anatomically informed basis functions for EEG source localization: combining functional and anatomical constraints. *Neuroimage* 16:678–695
49. Phillips C, Rugg MD, Friston KJ (2002) Systematic regularization of linear inverse solutions of the EEG source localization problem. *Neuroimage* 17:287–301
50. Yao D, He B (2001) A self-coherence enhancement algorithm and its application to enhancing three-dimensional source estimation from EEGs. *Ann Biomed Eng* 29:1019–1027
51. de Tommaso M, Difruscolo O, Sciruicchio V, Specchio N, Livrea P (2007) Abnormalities of the contingent negative variation in Huntington's disease: correlations with clinical features. *J Neurol Sci* 254:84–89
52. Beste C, Saft C, Andrich J, Gold R, Falkenstein M (2008) Response inhibition in Huntington's disease—a study using ERPs and sLORETA. *Neuropsychologia* 46:1290–1297
53. Huntington Study Group (1996) Unified Huntington's disease rating scale: reliability and consistency. *Mov Disord* 11:136–142
54. Folstein MF, Folstein SE, McHugh PR (1975) "Mini-mental state". A practical method for grading the cognitive state of patients for the clinician. *J Psychiatr Res* 12:189–198
55. Shoulson I, Fahn S (1979) Huntington disease: clinical care and evaluation. *Neurology* 29:1–3
56. Anderer P, Semlitsch HV, Saletu B, Barbanj MJ (1992) Artifact processing in topographic mapping of electroencephalographic activity in neuropsychopharmacology. *Psychiatry Res* 45:79–93
57. Anderer P, Saletu B, Kinsperger K, Semlitsch H (1987) Topographic brain mapping of EEG in neuropsychopharmacology—Part I. Methodological aspects. *Methods Find Exp Clin Pharmacol* 9:371–384
58. Kubicki S, Herrmann WM, Fichte K, Freund G (1979) Reflections on the topics: EEG frequency bands and regulation of vigilance. *Pharmakopsychiatr Neuropsychopharmakol* 12:237–245
59. Ary JP, Klein SA, Fender DH (1981) Location of sources of evoked scalp potentials: corrections for skull and scalp thicknesses. *IEEE Trans Biomed Eng* 28:447–452
60. Talairach J, Tournoux P (1988) Co-planar stereotaxic atlas of the human brain. Thieme, Stuttgart
61. Towle VL, Bolanos J, Suarez D, Tan K, Grzeszczuk R, Levin DN, Cakmur R, Frank SA, Spire JP (1993) The spatial location of EEG electrodes: locating the best-fitting sphere relative to cortical anatomy. *Electroencephalogr Clin Neurophysiol* 86:1–6
62. Holmes AP, Blair RC, Watson JD, Ford I (1996) Nonparametric analysis of statistic images from functional mapping experiments. *J Cereb Blood Flow Metab* 16:7–22
63. Friston K (1996) Statistical parametric mapping and other analyses of functional imaging data. In: Tago AW, Mazziotta JC (eds) *Brain Mapping*. Academic Press, San Diego, pp 363–386
64. Cross EM, Chaffin WW (1982) Use of the binomial theorem in interpreting results of multiple tests of significance. *Educ Psychol Measurement* 42:25–34
65. Babiloni C, Binetti G, Cassetta E, Cerboneschi D, Dal Forno G, Del Percio C, Ferreri F, Ferri R, Lanuzza B, Miniussi C, Moretti DV, Nobili F, Pascual-Marqui RD, Rodriguez G, Romani GL, Salinari S, Tecchio F, Vitali P, Zanetti O, Zappasodi F, Rossini PM (2004) Mapping distributed sources of cortical rhythms in mild Alzheimer's disease. A multicentric EEG study. *Neuroimage* 22:57–67
66. Hughes SW, Crunelli V (2005) Thalamic mechanisms of EEG alpha rhythms and their pathological implications. *Neuroscientist* 11:357–372
67. Alper KR, John ER, Brodie J, Gunther W, Daruwala R, Prichep LS (2006) Correlation of PET and qEEG in normal subjects. *Psychiatry Res* 146:271–282
68. Head H (1923) The conception of nervous and mental energy. II. Vigilance: a physiological state of the nervous system. *Br J Psychol* 14:125–147
69. Bente D (1977) Vigilance: psychophysiological aspects. *Verh Dtsch Ges Inn Med* 83:945–952
70. Saletu B, Grunberger J (1985) Memory dysfunction and vigilance: neurophysiological and psychopharmacological aspects. *Ann N Y Acad Sci* 444:406–427
71. Anokhin AP, Birbaumer N, Lutzenberger W, Nikolaev A, Vogel F (1996) Age increases brain complexity. *Electroencephalogr Clin Neurophysiol* 99:63–68
72. Polich J (1997) EEG and ERP assessment of normal aging. *Electroencephalogr Clin Neurophysiol* 104:244–256
73. Holschneider DP, Leuchter AF (1995) Beta activity in aging and dementia. *Brain Topogr* 8:169–180
74. Gawel M, Zalewska E, Szmidt-Salkowska E, Kowalski J (2009) The value of quantitative EEG in differential diagnosis of Alzheimer's disease and subcortical vascular dementia. *J Neurol Sci* 283:127–133
75. Saletu B, Anderer P, Paulus E, Grunberger J, Wicke L, Neuhold A, Fischhof PK, Litschauer G (1991) EEG brain mapping in diagnostic and therapeutic assessment of dementia. *Alzheimer Dis Assoc Disord* 5(Suppl 1):57–75
76. Muhlau M, Weindl A, Wohlschlagel AM, Gaser C, Stadler M, Valet M, Zimmer C, Kassubek J, Peinemann A (2007) Voxel-based morphometry indicates relative preservation of the limbic prefrontal cortex in early Huntington disease. *J Neural Transm* 114:367–372
77. Thiruvady DR, Georgiou-Karistianis N, Egan GF, Ray S, Sritharan A, Farrow M, Churchyard A, Chua P, Bradshaw JL, Brawn TL, Cunnington R (2007) Functional connectivity of the prefrontal cortex in Huntington's disease. *J Neurol Neurosurg Psychiatry* 78:127–133
78. Dursun SM, Burke JG, Andrews H, Mlynik-Szmid A, Reveley MA (2000) The effects of antipsychotic medication on saccadic eye movement abnormalities in Huntington's disease. *Prog Neuropsychopharmacol Biol Psychiatry* 24:889–896
79. Schmidtke K, Manner H, Kaufmann R, Schmolck H (2002) Cognitive procedural learning in patients with fronto-striatal lesions. *Learn Mem* 9:419–429
80. Bonelli RM, Cummings JL (2008) Frontal-subcortical dementias. *Neurologist* 14:100–107
81. Joel D (2001) Open interconnected model of basal ganglia-thalamocortical circuitry and its relevance to the clinical syndrome of Huntington's disease. *Mov Disord* 16:407–423
82. Alexander GE, DeLong MR, Strick PL (1986) Parallel organization of functionally segregated circuits linking basal ganglia and cortex. *Annu Rev Neurosci* 9:357–381
83. Alexander GE, Crutcher MD (1990) Functional architecture of basal ganglia circuits: neural substrates of parallel processing. *Trends Neurosci* 13:266–271
84. Vonsattel JP, Myers RH, Stevens TJ, Ferrante RJ, Bird ED, Richardson EP Jr (1985) Neuropathological classification of Huntington's disease. *J Neuropathol Exp Neurol* 44:559–577

85. Hedreen JC, Folstein SE (1995) Early loss of neostriatal striosome neurons in Huntington's disease. *J Neuropathol Exp Neurol* 54:105–120
86. Alper K, Gunther W, Prichep LS, John ER, Brodie J (1998) Correlation of qEEG with PET in schizophrenia. *Neuropsychobiology* 38:50–56
87. Gavazzi C, Nave RD, Petralli R, Rocca MA, Guerrini L, Tessa C, Diciotti S, Filippi M, Piacentini S, Mascalchi M (2007) Combining functional and structural brain magnetic resonance imaging in Huntington disease. *J Comput Assist Tomogr* 31:574–580
88. Muhlau M, Gaser C, Wohlschlagel AM, Weindl A, Stadler M, Valet M, Zimmer C, Kassubek J, Peinemann A (2007) Striatal gray matter loss in Huntington's disease is leftward biased. *Mov Disord* 22:1169–1173